"Designing Out" Disulfide Bonds: Thermodynamic Properties of 30−51 Cystine Substitution Mutants of Bovine Pancreatic Trypsin Inhibitor†

Yi Liu,‡,§ Kenneth Breslauer,*,§,|| and Stephen Anderson*,‡,§,⊥

Center for Advanced Biotechnology and Medicine, 679 Hoes Lane, Piscataway, New Jersey 08854-5638, Department of Chemistry, Rutgers University, P.O. Box 939, Piscataway, New Jersey 08855-0939, The Cancer Institute of New Jersey, New Brunswick, New Jersey 08901, and Department of Molecular Biology and Biochemistry, Rutgers University, New Brunswick, New Jersey 08903

Received September 25, 1996; Revised Manuscript Received January 27, 1997⊗

ABSTRACT: We have used a combination of spectroscopic and calorimetric techniques to assess the thermodynamic and extrathermodynamic consequences of paired amino acid substitutions at positions 30 and 51 in bovine pancreatic trypsin inhibitor (BPTI). Correctly folded, wild type BPTI contains a disulfide at the 30−51 positions, with the nonbackbone atoms of this cystine being relatively solvent inaccessible. Mutants missing this buried 30−51 disulfide adopt a conformation very similar to that of the native state of wild type BPTI (Eigenbrot et al., 1990, 1992), although they are severely destabilized relative to the wild type molecule (Hurle et al., 1990). We have conducted a systematic effort to find the energetically most favorable substitution for this buried 30−51 disulfide in BPTI. To this end, we have studied and characterized the thermally induced and guanidine hydrochloride-induced denaturation transitions for a family of mutants in which the amino acid residue(s) at positions 30 and/or 51 have been systematically altered. Specifically, we studied the unfolding transitions of the following series of residue 30/residue 51 paired substitution mutants: C30A/C51A, C30V/C51A, C30G/C51A, C30S/C51A, C30T/C51A, C30A/C51S, C30S/C51S, and C30G/C51M. For this series of mutants, comparisons between the relative stabilization free energies, derived from analysis of the denaturation profiles, allow us to reach the following conclusions: (a) side chains containing polar moieties (Ser and Thr) are destabilizing, with this effect being position dependent (i.e., a serine substitution is more destabilizing at position 51 than at position 30); (b) the destabilizing effects of two serine substitutions are approximately additive, suggesting that side chain−side chain hydrogen bonds between the two serine hydroxyl groups probably are weak or nonexistent; (c) the thermodynamic impact of a Gly30 substitution is consistent with a glycine-induced increase in the configurational entropy of the unfolded state; (d) the C30G/C51M mutant is highly destabilized relative to the C30A/C51A mutant despite the fact that, based on considerations of hydrophobicity and steric fit, substitution of a buried disulfide by Gly30 and Met51 would be expected to be optimal. Methionine may be particularly ill-suited as a buried disulfide substitute due to the large loss of side chain conformational entropy it undergoes during the transition from the unfolded to the native state. In the aggregate, our data provide insight into the residue-, position-, and context-dependent consequences on protein stability of "designing out" the buried 30−51 disulfide bond in the BPTI molecule. These data also suggest that a previously unrecognized component of disulfide bridge stabilization of proteins is the relatively minor penalty in side chain conformational entropy incurred by cystine residues during folding due to their severely restricted rotation even in the unfolded state.

The interiors of proteins are generally tightly packed. Such packing efficiently excludes solvent and, through van der Waals and hydrophobic interactions, makes a significant contribution to the stabilization of native conformations (Ponder & Richards, 1987; Lim & Sauer, 1989; Lim et al., 1992; Kellis et al., 1989; Shortle et al., 1990; Chothia, 1975; Richards, 1974, 1977; Eriksson et al., 1992; Garvey & Matthews, 1989; Jackson et al., 1993; Dao-pin et al., 1991; Blaber et al., 1993; Dill, 1990; Richards & Lim, 1994). Core mutations which result in polar substitutions often are destabilizing, even if they do not violate packing considerations. This feature reflects the unfavorable free energy consequences of burying charges and/or unsatisfied hydrogen bonds in a highly hydrophobic environment (Lim & Sauer, 1989; Lim et al., 1992; Blaber et al., 1993; Dao-pin et al., 1991; Hurle et al., 1990; Serrano et al., 1992; Ladbury et al., 1995; Liu, Breslauer, and Anderson, unpublished observations).

In wild type bovine pancreatic trypsin inhibitor (BPTI),[1] the 30−51 disulfide bond extends through the hydrophobic core of the molecule. We previously have used Gdn-HCl-

† This work was supported by National Institutes of Health Grants GM23509 and GM34469 (K.B.) and AG10462 and AG11525 (S.A.).

* Authors to whom correspondence should be addressed.
‡ Center for Advanced Biotechnology and Medicine.
§ Department of Chemistry, Rutgers University.
|| The Cancer Institute of New Jersey.
⊥ Department of Molecular Biology and Biochemistry, Rutgers University.

⊗ Abstract published in *Advance ACS Abstracts,* April 1, 1997.

[1] Abbreviations: BPTI, bovine pancreatic trypsin inhibitor; Gdn-HCl, guanidine hydrochloride; CD, circular dichroism; EDTA, ethylenediaminetetraacetic acid; DTT, dithiothreitol; DSC, differential scanning calorimetry; T_m, midpoint temperature of the thermal melting transition; $C_{1/2}$, midpoint concentration of denaturant in equilibrium unfolding; NMR, nuclear magnetic resonance spectroscopy.

S0006-2960(96)02423-3 CCC: $14.00

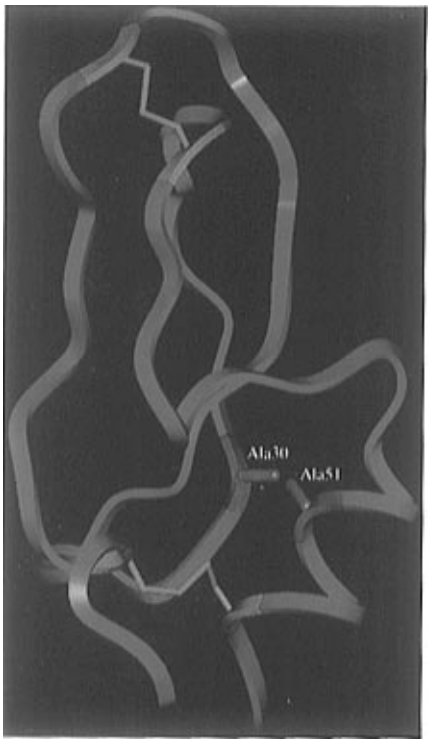

FIGURE 1: Backbone representation of [C30A/C51A]BPTI adapted from the X-ray structure (Eigenbrot et al., 1990).

mediated denaturation to show that mutants of BPTI which lack this disulfide bond are destabilized and exhibit altered rates of folding and unfolding relative to wild type BPTI (Hurle et al., 1990, 1991). The degree of this destabilization is dependent on the nature of the 30−51 cystine substitution (Hurle et al., 1990), and the substitutions induce only minor perturbations in the folded conformation of BPTI (Eigenbrot et al., 1990, 1992; Staley & Kim, 1992; Mierlo et al., 1991; Ferrer et al., 1995). These results suggest that different amino acid side chains inserted in place of the buried, solvent-inaccessible 30−51 disulfide can have significant thermodynamic consequences even when they induce relatively few detectable structural alterations in the native state. The fact that apparently isostructural native states are not isoenergetic is not surprising since, as recently emphasized by Sturtevant (1994), this observation could reflect (i) differences in the native states which are below the detectability limits of NMR or X-ray methods (including hydration), (ii) steric constraints, (iii) the hydrophobic nature of the local environment, and (iv) substitution-mediated differences in the final unfolded states.

To investigate these effects further and to explore possible compensating changes that might ameliorate the effects of such destabilizing disulfide mutations (effectively attempting to "engineer" stability back into the molecule), we have examined a series of BPTI Cys30/Cys51 substitutions. The buried nature of the 30−51 disulfide and concomitant packing constraints limit the number of candidate residue pairs to those having relatively small side chains, consistent with the elongated and narrow cavity in the hydrophobic core left by removal of the 30−51 disulfide. Using the C30A/C51A BPTI mutant as our reference, which has the crystal structure shown in Figure 1, we have replaced Ala30 and Ala51 by the following pairs of amino acids: Gly30/Ala51, Val30/Ala51, Thr30/Ala51, Ser30/Ala51, Ala30/Ser51, Ser30/Ser51, and Gly30/Met51. These substitutions, which occupy the positions of the two half-cystines that comprise the 30−51 disulfide bond, differ in shape, volume, and polarity. We have used differential scanning calorimetry and guanidine hydrochloride-mediated denaturation to characterize the unfolding transitions of this family of BPTI mutants in an effort to assess the effects of packing, polarity, and compensation on protein stability when these amino acids substitute for a buried disulfide bond.

MATERIALS AND METHODS

Chemicals. Guanidine hydrochloride (Gdn-HCl) solution was purchased from Pierce Biochemicals (ultrapure grade, Pierce, Rockford, IL) and used without further purification. Oligonucleotides were synthesized by the solid-phase phosphoramidite method.

Bacterial Strains and Vectors. *Escherichia coli* strains TG-1 and XL1-Blue (Stratagene, La Jolla, CA) were used for cloning and mutagenesis; *E. coli* strains W3110 and RV308 (Mauer et al., 1980) were used as the expression hosts. Plasmids pEZZ-BPTI(30−51) and pHAZY(30−51) have been previously described (Altman et al., 1991; Nilsson et al., 1991a,b). The plasmid pEZY-BPTI(30−51) was constructed from plasmids pEZZ-BPTI and pHAZY-BPTI-(30−51) as follows. After double digestion of both plasmids by restriction enzymes *Bgl*II and *Stu*I (New England Biolabs), the large fragment from plasmid pEZZ-BPTI (4482 base pairs) (Nilsson et al., 1991a,b) and the small fragment from plasmid pHAZY-BPTI (145 base pairs), containing the chymotrypsin cleavage site and a portion of the "Z" domain (Altman et al., 1991), were isolated and purified by polyacrylamide gel electrophoresis. The two fragments were joined by T4 DNA ligase (New England Biolabs) and used to transform *E. coli* TG1. The sequence of the resultant plasmid was confirmed by dideoxy DNA sequencing (Sanger et al., 1977).

Mutagenesis. Oligonucleotide-directed *in vitro* mutagenesis was performed on single-stranded plasmid DNA using synthetic oligonucleotides and standard procedures (Marks et al., 1987a,b; Sayers et al., 1988). Single-stranded DNA was prepared from plasmid pEZY-BPTI(30−51) as described by Vieira and Messing (1987). The gene coding for BPTI mutant C30A/C51A was used as the basis for subsequent mutations. Positive mutant colonies were restreaked, and the entire protein coding region in the plasmids isolated from these was checked by DNA sequencing to confirm the presence of the desired mutation and rule out the presence of adventitious mutations.

Expression of BPTI Variants. Mutants C30S/C51A, C30G/C51A, and C30A/C51S were expressed in a periplasmic expression system (Nilsson et al., 1991a). *E. coli* strains W3110 and RV308 were transformed with various pEZY-BPTI expression plasmids encoding the BPTI variant. Transformants were selected on LB agar plates with 50 μg/mL ampicillin. Seed cultures (10 mL) were grown for approximately 16 h at 30 °C. Seed cultures were then spun down and the cells washed by resuspending them in 1 mL of fresh medium. Washed cells were used to inoculate 2 L of fresh 2XYT medium (Sambrook et al., 1989) supplemented with 0.2% glucose and 250 mg/L ampicillin and grown in four 2000 mL baffled shake flasks (500 mL in each flask) at 30 °C for 20 h. Cells were harvested by centrifugation at 8000*g* for 20 min.

The C30A/C51A, C30V/C51A, and C30T/C51A BPTI mutants were expressed in a secretion system under control of the STII leader sequence, as previously described (Marks et al., 1987).

BPTI mutants poorly expressed in a secretion system can be produced in sufficient quantities using an intracellular expression vector, pHAZY-BPTI (Altman et al., 1991). Due to the inability to express disulfide mutants C30S/C51S and C30G/C51M in large amounts using secretion systems, these two mutants were expressed using a similar intracellular expression system. The coding sequences for mutants C30S/C51S and C30G/C51M were inserted into plasmid pHAZY. Saturated overnight seed cultures of bacteria in 2XTY were diluted 25-fold into 2XTY media supplemented with 250 mg/L ampicillin and 0.2% glucose and grown at 37 °C. Expression of recombinant fusion protein was induced at mid-log phase by addition of 25 mg/mL β-indoleacrylic acid to a final concentration of 20 mg/L. When expressed in this system, fusion proteins are sequestered in inclusion bodies, which inhibit proteolytic degradation in the cytoplasm, and thus the full-length fusion proteins can be obtained.

The expression yields of BPTI mutants were measured by activity analysis using a trypsin inhibition assay as described by Marks (1986). The assay was performed in 0.2 M triethanolamine (pH 7.8), 10 mM $CaCl_2$, and 0.4 mg/mL N^{α}-benzoyl-DL-arginine-*p*-nitroanilide (BAPA) at 25 °C with 50 μL of cell extract and 10 μg of bovine trypsin in 1 mL final volume.

Purification of BPTI Mutants. For mutants expressed as protein A fusions in the periplasmic expression systems, purification was carried out as follows. After the cells were harvested, an osmotic shock was performed to release periplasmic proteins (Nilsson & Abrahmsen, 1990). Cells from a 1 L culture were suspended in 20 mL of 0.1 M sucrose buffer (0.1 M Tris-HCl, pH 8.0, 0.5 M sucrose, 2 mM EDTA) and incubated for 10 min on ice. Then 250 mL of lysozyme (100 mg/mL) and 20 mL of ice-cold water were added, and the mixture was incubated on ice for an additional 5 min. The osmotically shocked cells were centrifuged at 10000*g* for 20 min at 4 °C, and the supernatant of the centrifugation was taken as the periplasmic fraction. This fraction was filtered through a 0.45 μm filter.

A chymotrypsin affinity column was prepared by immobilizing chymotrypsin on Affi-Gel 10 (Bio-Rad) as previously described (Marks et al., 1986). The filtrate of the periplasmic extract was loaded onto a chymotrypsin column of a size sufficient to bind all the BPTI; the column was preequilibrated with 50 mM Tris-HCl (pH 7.4), 150 mM NaCl, and 0.05% Tween 20 (TST buffer) at 4 °C and washed after BPTI binding with 10 column volumes of TST buffer. Following the wash, 0.5 volume of TST and 20 μL of chymotrypsin solution (15 mg/mL) were added to the column. The column was sealed and incubated on a gentle rocker at 4 °C overnight to allow the cleavage of the linker between the Z domain and BPTI. After cleavage, the column was washed with 5 volumes of TST buffer, followed by 2 volumes of 50 mM ammonium acetate (pH 5.0), to flush out the cleaved Z domain. The BPTI was eluted with 0.1 M acetic acid (pH 2.5) and lyophilized.

Mutant BPTIs were further purified by cation-exchange chromotography using a 10/10 Mono S FPLC column (Pharmacia), with a gradient from buffer A (50 mM acetic acid titrated to pH 4.0 using ammonium acetate) to buffer B (5 M acetic acid titrated to pH 4.0 using ammonium acetate), or an Applied Biosystems Aquapore CX-300 HPLC column with a gradient from 0.1 M ammonium acetate (buffer A) to 1.0 M ammonium acetate (buffer B) at pH 6.0. Flow rates were 0.5 mL/min. After cation-exchange chromatography, all the BPTI mutants were subjected to buffer exchange using a Sephadex G-25 or Bio-Rad PD-10 column in 50 mM ammonium bicarbonate (pH 7.8) and lyophilized. Purified BPTI mutants were stored as a powder at −20 °C.

For mutants S30/S51 and G30/M51, expressed using the intracellular expression vector pHAZY-BPTI, purification was by the method of Kim et al. (1997). Briefly, after the cells were harvested by centrifugation at 8000*g* for 20 min, cell pellets were resuspended in one-tenth culture volume of lysis buffer containing 10 mM Tris-HCl (pH 7.8), 0.5% Triton X-100, and 1 mM EDTA and lysed by sonication. The cell lysate was centrifuged at 10000*g* for 20 min at 4 °C. The pellet, which contained the inclusion bodies, was dissolved in 50 mL of 7 M Gdn-HCl in 10 mM Tris-HCl (pH 7.8). The dissolved inclusion bodies were reduced by addition of DTT to a final concentration of 20 mM with 1 h of incubation at room temperature and centrifuged at 16000*g* for 20 min at 4 °C. The supernatant was acidified by adding HCl to a final concentration of 15 mM and dialyzed against 10 mM HCl and 0.1 mM DTT overnight. The dialysate was centrifuged at 16000*g* for 50 min at 4 °C, and 7 M Gdn-HCl was added to the supernatant to adjust the final concentration of Gdn-HCl to 1.1 M. The supernatant was neutralized with 1 M Tris-HCl to pH 7.5, clarified by passing it through a 0.45 μm filter, and loaded onto an IgG−Sepharose column (Pharmacia) preequilibrated with 1 M Gdn-HCl. The column was washed with 5 volumes of 1 M Gdn-HCl, followed by 3 volumes of refolding buffer containing 100 mM Tris-HCl (pH 8.7), 200 mM KCl, 10 mM GSH, and 1 mM GSSG, and then incubated at 4 °C for at least 20 h to allow refolding to occur. After the column was washed with 50 mM ammonium acetate, the refolded fusion proteins were eluted at 4 °C with 0.5 M acetic acid titrated to pH 3.3 by ammonium acetate. Final purification of the protein was as described above.

The purity of all the BPTI mutants was verified by SDS−polyacrylamide gel electrophoresis, reverse-phase HPLC chromatography on a Vydac C4 peptide/protein column (4.6 mm × 25 cm), N-terminal Edman degradation, amino acid analysis, and mass spectrometry. All the mutant polypeptides exhibited the expected amino acid composition and mass, had no detectable internal cleavages, and were of a purity greater than or equal to 95%. Wild type BPTI standards, where used, were derived from either recombinant (Marks et al., 1986) or natural (aprotinin) sources.

Sample Preparation. The buffer used for all studies was 10 mM potassium phosphate, 0.1 M sodium chloride (NaCl), and 0.2 mM disodium ethylenediaminetetraacetate (EDTA). Sample solutions were prepared immediately before use by dissolving the protein in buffer solution with the appropriate pH. The solution concentrations of wild type and mutant BPTIs were determined spectrophotometrically at 25 °C using a Perkin-Elmer lamda 4C UV/vis spectrophotometer. The absorbance of the wild type BPTI solution was measured at 280 nm, and the concentration was calculated using an extinction coefficient of $\epsilon_{280} = 5400\ M^{-1}\ cm^{-1}$ [AS(0.1%,

280) unit = 0.83] (Kassell, 1970). The absorbances of all the mutant samples were measured similarly. The concentrations of mutants were also determined by measuring tyrosine and cysteine absorbance of the unfolded proteins (Edelhoch, 1967; Staley & Kim, 1992), and these agreed well with the values obtained from absorbance measurements at 280 nm in the native proteins.

Differential Scanning Calorimetry. Excess heat capacity versus temperature melting profiles for the BPTI mutants (except C30S/C51S and C30G/C51M) were determined using a model MC-2 differential scanning calorimeter (Microcal, Amherst, MA). Protein concentrations for these measurements varied between 0.35 and 1.0 mg/mL. Prior to each measurement the buffer and sample solutions were filtered through 0.45 μm microfilters and degassed under aspirator vacuum. Each protein scan was preceded by a buffer versus buffer scan to establish a base line. The transitions of the wild type (Schwarz et al., 1987) and mutant BPTI's were found to be independent of scan rate. Consequently, all measurements were carried out with a constant heating rate of 60 °C/h, with the excess heat capacity, C_p, being recorded continuously from 0 to 100 °C. Each sample solution was subjected to up to five heating and cooling cycles to ascertain the reversibility of the protein transition(s). At neutral pH the transitions were irreversible, but they were partially reversible at lower pHs. Kim et al. (1993) have reported the hydrolysis of peptide bonds of their BPTI mutants in calorimetry measurements. However, from our DSC measurements, we did not see any evidence of pH-dependent thermally induced hydrolysis for our BPTI mutants. All measurements were performed with an excess pressure of 1 atm. The excess heat capacity (ΔC_p) and temperature (T) data were collected at intervals of 0.1 °C. The transition enthalpy was derived from the area under the ΔC_p versus T curve. The shape of this melting profile also was analyzed using eq 1 to obtain a model-dependent van't Hoff enthalpy of unfolding (Davaloo & Crothers, 1976):

$$H_{VH} = \frac{B}{1/T_1 - 1/T_2} \quad (1)$$

In this equation, T_1 and T_2 are the temperatures below and above T_{max} at which C_p is half of its height at T_{max}, and B is a constant which is dependent on the molecularity of the process under investigation (Marky & Breslauer, 1987; Breslauer, 1994, 1995). For a monomolecular process, such as BPTI unfolding, $B = 7$.

Circular Dichroism. All circular dichroism (CD) spectroscopy measurements were performed on an AVIV Model 60DS spectropolarimeter equipped with a thermoelectrically controlled cell holder. A rectangular quartz cuvette (Hellma) with 0.1 cm path length was used. The CD spectra before and after the thermally induced denaturations of the wild type and all the mutant BPTI molecules were collected over a range of pH values. Protein concentrations prepared for CD measurements were approximately 0.15 mg/mL.

Thermal Denaturation. CD ellipticities at two wavelengths, 222 and 205 nm, were measured as a function of temperature. The resulting denaturation curves were analyzed assuming a two-state model. This assumption is consistent with our calorimetric results, since, within experimental error, the van't Hoff and calorimetric transition enthalpies are equal. The van't Hoff transition enthalpies, ΔH_{VH}, at T_m were calculated from the CD melting curves using the equation (Marky & Breslauer, 1987; Breslauer, 1994, 1995):

$$\Delta H_{VH} = (2 + 2n)RT^2(d\alpha/dT)_{T_m} \quad (2)$$

where n is the molecularity of the transition, T_m is defined as the midpoint temperature of the thermal unfolding transition, and α is the fractional extent of reaction. For BPTI and its mutants, $n = 1$.

CD-monitored thermal denaturation curves also were determined at different hydrogen ion concentrations to calculate the pH dependence of ΔH_{VH}. These thermal denaturations were performed at protein concentrations of approximately 0.15 mg/mL. The buffer was 10 mM potassium phosphate, 0.1 M NaCl, and 0.2 mM EDTA. The ellipticity was measured at 1 °C intervals at a heating rate of 1 °C/min. The signal was averaged for 30 s. For most mutants, the ellipticity was collected from 0 ~100 °C. The resulting thermal denaturation profiles were found to be irreversible at pH 7 and partially reversible at lower pHs.

Equilibrium Unfolding with Guanidine Hydrochloride. Guanidine hydrochloride-(Gdn-HCl-) induced denaturation of BPTI was monitored by CD spectroscopy. The ellipticity at 222 nm was measured as a function of Gdn-HCl concentration at 25 °C. Assuming a two-state model, the fraction of unfolded protein, F_u, was calculated using the equation (Pace, 1975):

$$F_u = (q_f - q_{obs})/(q_f - q_u) \quad (3)$$

where q_{obs} is the observed ellipticity and q_f and q_u are the ellipticities of the folded and unfolded conformations, which are assumed to vary linearly with Gdn-HCl concentration. From these data, the equilibrium constant, K, and the difference in free energy between the folded and unfolded conformations, ΔG, were calculated using the relationships:

$$K = F_u/(1 - F_u) = (q_f - q_{obs})/(q_{obs} - q_u) \quad (4)$$

$$\Delta G = -RT \ln K = -RT \ln[(q_f - q_{obs})/(q_{obs} - q_u)] \quad (5)$$

The change in free energy so calculated between the folded and unfolded conformations also can be expressed as a linear function of the denaturant concentration (Pace, 1975; Schellman, 1978):

$$\Delta G = \Delta G^\circ - m[\text{Gdn-HCl}] \quad (6)$$

where ΔG° represents, at a given temperature and pH, the difference in free energy between the native and unfolded forms in the absence of denaturant, while the parameter m represents the dependence of the free energy of unfolding on denaturant concentration. The midpoint of the transition, $C_{1/2}$, is the concentration of the denaturant at which half of the protein is unfolded. We obtained values for the unfolding free energy (ΔG°) in the absence of Gdn-HCl, as well as m, the slope of the curve which relates ΔG to the denaturant concentration, from nonlinear least squared fits of the denaturant-induced CD unfolding curves using the equation (Lim et al., 1992; Pace et al., 1990; Santoro & Bolen, 1988):

$$\Theta_{222} = \left[(a_f[\text{Gdn-HCl}] + b_f) + (a_u[\text{Gdn-HCl}] + b_u)\exp\left(-\frac{\Delta G^\circ - m[\text{Gdn-HCl}]}{RT}\right)\right] \Big/ \left[1 + \exp\left(-\frac{\Delta G^\circ - m[\text{Gdn-HCl}]}{RT}\right)\right] \quad (7)$$

In this equation, a_f is the slope of the native state base line, b_f is the ellipticity of the native state at 0 M Gdn-HCl (the intercept of the pretransition base line), a_u is the slope of the posttransition base line, and b_u is the ellipticity of the unfolded state at 0 M Gdn-HCl.

In all the Gdn-HCl-induced denaturation experiments, sample solutions were prepared by adding equal volumes of stock protein solution into a standard buffer (10 mM potassium phosphate, 0.1 M NaCl, 0.2 mM EDTA, pH 7.0) containing various concentrations of Gdn-HCl. The resulting solutions contained 0.15−0.2 mg/mL protein with the desired denaturant concentration. All sample solutions with different concentrations of Gdn-HCl were incubated at 25 °C for 2 h to ensure equilibrium. Each sample then was transferred to a 1 mm path length quartz cuvette, and the ellipticity at 222 nm was measured. For each sample, blank solutions with identical Gdn-HCl concentrations in the standard buffer also were measured, and the background ellipticity was subtracted. The measured ellipticities for each mutant were converted to molar ellipticities, and the data were fitted to eq 7.

Calculation of Water-Accessible Surface Areas. To evaluate correlations between changes in the water-accessible surface area of the protein and the ΔC_p of protein unfolding, we calculated the changes in water-accessible nonpolar and polar surface areas arising from the denaturation of each 30−51 disulfide mutant. The coordinates for the crystal structure of mutant C30A/C51A (Eigenbrot et al., 1990) obtained from the Brookhaven Protein Data Base (file name 7PTI. PDB) were used to model the native states. To model the denatured states, random coil structures for all the mutants were built from primary amino acid sequences using the IMPACT program kindly provided by Dr. R. Levy of the Rutgers Chemistry Department (Kitchen et al., 1990). The water-accessible surface areas of the native and denatured mutant states then were calculated using the program ACCESS (Lee & Richards, 1971) with a water molecule of radius 1.4 Å as the probe. The program ACCFMT was used to sum the total nonpolar and polar surface areas for each mutant. In this program, carbon is considered to be a nonpolar atom, and oxygen, nitrogen, and sulfur are defined as polar atoms.

RESULTS

CD Spectroscopy of the Native States of the 30−51 Disulfide Substitution Mutants. Panel A of Figure 2 shows the circular dichroism spectra at pH 7 and 25 °C for wild type BPTI and a series of mutants having different substitutions at residues 30 and 51. Note that the CD spectra for the C30A/C51A (open circles), C30V/C51A (filled diamonds), and C30T/C51A (open diamonds) mutants are virtually superimposable, with the spectra for the other 30−51 mutants being quite similar. Compared with wild type BPTI, the intensities of the ellipticity minima at 202−205 nm are somewhat reduced, but the qualitative shapes of the spectra remain the same. Aromatic residues in the hydrophobic core of BPTI are known to contribute significantly to its CD spectrum [Manning & Woody, 1989; see also Chakrabartty et al. (1993) and Vuilleumier et al. (1993)], so it is not unexpected that removal of the buried 30−51 disulfide would affect the packing of these residues and thus perturb the CD spectrum. However, based on the similarity of these spectra, the CD-detectable secondary structural features of the mutant and wild type BPTI conformations appear not to be substantially different from each other. This conclusion is consistent with previous X-ray and NMR structural studies on three of these mutants ([C30A/C51A], [C30V/C51A], and [C30T/C51A]) which revealed that they exhibit native-like folds (Eigenbrot et al., 1990, 1992; Hurle et al., 1992). Thus, in the absence of denaturant, we conclude that at neutral pH and low temperature the mutants shown in panel A of Figure 2 assume predominantly native-like conformations. This is consistent with the fact that all mutants were fully active as trypsin inhibitors (data not shown).

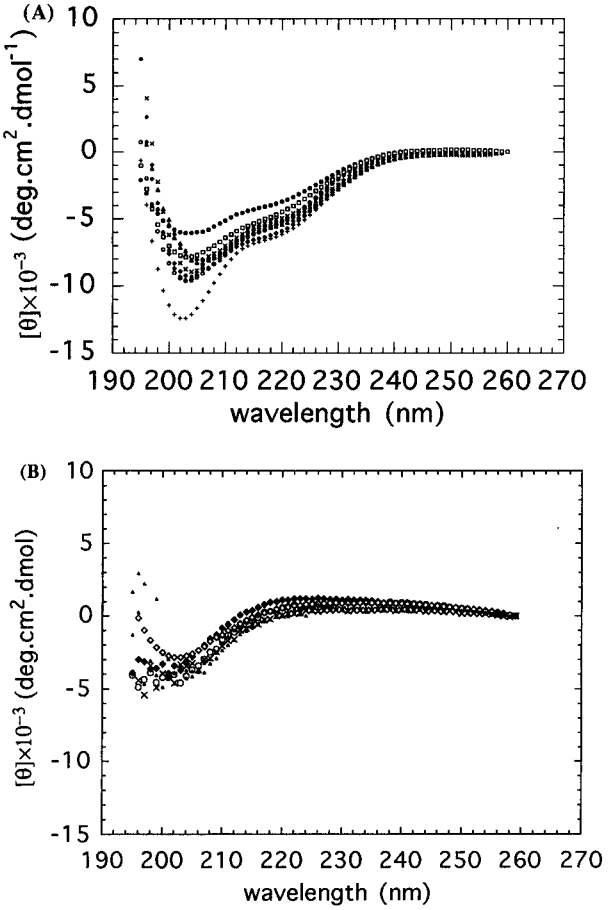

FIGURE 2: (A) CD spectra of native wild type and 30−51 disulfide mutants of BPTI: wild type (+); C30A/C51A (open circles); C30V/C51A (filled diamonds); C30G/C51A (open triangles); C30T/C51A (open diamonds); C30S/C51A (filled triangles); C30A/C51S (×); C30S/C51S (filled circles); C30G/C51M (open squares). The spectra were measured at 25 °C in 10 mM potassium phosphate (pH 7.0) and 100 mM NaCl. (B) CD spectra of denatured 30−51 disulfide mutants of BPTI: C30A/C51A (open circles); C30V/C51A (filled diamonds); C30G/C51A (open triangles); C30T/C51A (open diamonds); C30S/C51A (filled triangles); C30A/C51S (×). All the mutants were denatured by heating to 95 °C. The spectra were measured at 95 °C in 10 mM potassium phosphate (pH 7.0) and 100 mM NaCl.

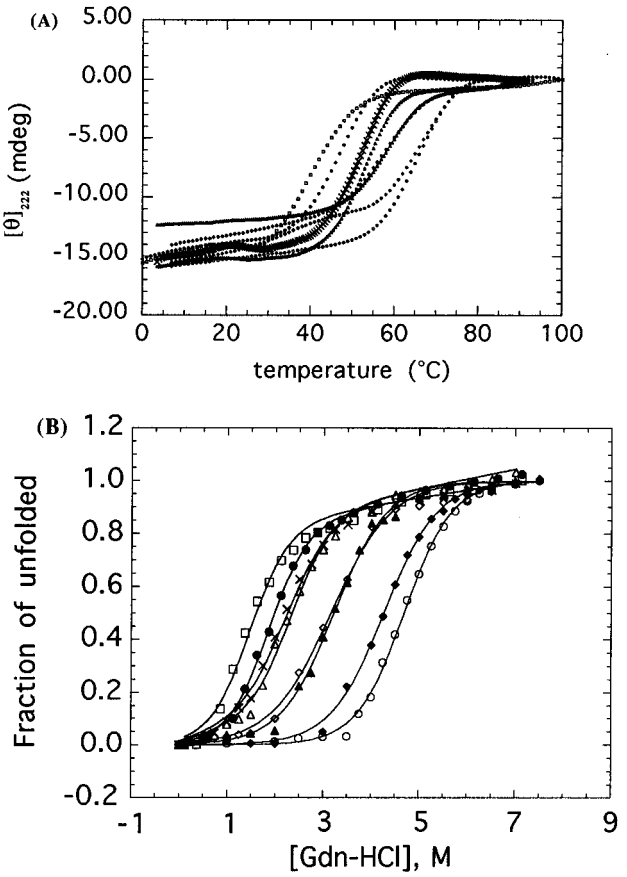

FIGURE 3: (A) Thermal denaturation of 30−51 disulfide mutants of BPTI as measured by CD spectroscopy at 222nm in 10 mM potassium phosphate (pH 7.0) and 100 mM NaCl: C30A/C51A (open circles); C30V/C51A (filled diamonds); C30G/C51A (open triangles); C30T/C51A (open diamonds); C30S/C51A (filled triangles); C30A/C51S (×); C30S/C51S (filled circles); C30G/C51M (open squares). (B) Guanidine hydrochloride-induced equilibrium unfolding of 30−51 disulfide mutants of BPTI: C30A/C51A (open circles); C30V/C51A (filled diamonds); C30G/C51A (open triangles); C30T/C51A (open diamonds); C30S/C51A (filled triangles); C30A/C51S (×); C30S/C51S (filled circles); C30G/C51M (open squares). Unfolding was monitored by CD spectroscopy at 222 nm, in 10 mM potassium phosphate (pH 7.0) and 100 mM NaCl, at 25 °C. The plots show the normalized data (fraction of unfolded) corrected for the slope of the base lines. The solid lines are the best fit of the data to a two-state process.

CD Spectroscopy of the Denatured States of the 30−51 Disulfide Mutants. As shown in panel B of Figure 2, the CD spectra of all mutants are similar at high temperature (95 °C) and exhibit features characteristic of an unfolded polypeptide chain (Yang & Kubota, 1985). We also found the CD spectra of the mutants unfolded in 8 M guanidine hydrochloride (spectra not shown) to be similar to each other and to those obtained at high temperature in the absence of the denaturant. We therefore conclude that both temperature and denaturant produce similar unfolded final states.

Relative Stabilities of the 30−51 Disulfide Substitutions. Panel A of Figure 3 shows thermally induced denaturation profiles for the mutants studied here as monitored by the change in ellipticity at 222 nm. Although only shown at pH 7.0, each transition was monitored over a range of pH and analyzed assuming a two-state model (see Materials and Methods). The resulting T_m and ΔH_{VH} values at pH 7 are listed in Table 1. Inspection of the curves in panel A of Figure 3 and the T_m and ΔG data in Tables 1 and 2, respectively, reveals that the thermal and thermodynamic stabilities of all mutants, with the exception of C30V/C30A, are significantly reduced relative to the C30A/C51A reference mutant.

Table 1: Parameters Characterizing the Thermally Induced Unfolding of the 30−51 Disulfide BPTI Mutants, Monitored by CD at pH 7

mutants	T_m (°C)	ΔH_{vH}[c] (kcal/mol)	ΔC_p [kcal/(mol·deg)]
C30A/C51A[a]	66 ± 0.5	61.5 ± 3.0	0.84
C30V/C51A[b]	67 ± 0.5	57.2 ± 2.5	0.51
C30G/C51A[a]	53 ± 0.5	48.4 ± 2.5	0.24
C30T/C51A[b]	58 ± 0.5	50.3 ± 3.0	0.35
C30S/C51A[a]	57 ± 0.5	50.1 ± 3.0	0.50
C30A/C51S[a]	52 ± 0.5	44.2 ± 3.0	0.58
C30S/C51S[b]	46 ± 0.5	44.5 ± 3.0	0.50 (est)[d]
C30G/C51M[b]	40 ± 0.5	38.7 ± 3.0	0.50 (est)[d]

[a] At least two independent measurements were performed. Errors were obtained from the standard deviations. [b] Single measurements were performed. Errors were obtained from fitting. [c] From eq 2; see Materials and Methods. [d] Thermal melt experiments for these mutants were performed only at pH 7. Thus, the mean value of ΔC_p for the other six mutants [0.5 kcal/(mol·deg)] was used as an estimate for C30G/C51M and C30S/C51S.

Table 2: Parameters Characterizing the Gdn-HCl-Induced Unfolding of the 30−51 Disulfide BPTI Mutants, monitored by CD at pH 7 and 25 °C

mutants	$\Delta G°$ (kcal/mol)	m [kcal/(mol·M Gdn)]	$C_{1/2}$ (M Gdn·HCl)
C30A/C51A[a]	5.5 ± 0.3	1.32 ± 0.03	4.25
C30V/C51A[b]	6.6 ± 0.2	1.43 ± 0.05	4.72
C30G/C51A[a]	3.2 ± 0.2	1.38 ± 0.06	2.20
C30T/C51A[b]	4.5 ± 0.3	1.42 ± 0.08	3.25
C30S/C51A[a]	4.4 ± 0.2	1.47 ± 0.05	3.12
C30A/C51S[a]	3.4 ± 0.2	1.37 ± 0.05	2.23
C30S/C51S[b]	2.7 ± 0.2	1.42 ± 0.07	1.75
C30G/C51M[b]	2.1 ± 0.2	1.44 ± 0.05	1.20

[a] At least two independent measurements were performed. Errors were obtained from the standard deviations. [b] Single measurements were performed. Errors were obtained from fitting.

Panel B of Figure 3 shows the corresponding CD-monitored guanidine hydrochloride-induced denaturations of the 30−51 disulfide mutants. Each curve was fitted and analyzed by a two-state model using the nonlinear least squares approach described in Materials and Methods, although some of the less stable variants (e.g., C30S/C51S and C30G/C51M) showed deviation from ideal two-state behavior. Employing the generally used assumption that the change in free energy between the folded and unfolded conformations varies linearly with the denaturant concentration (Pace, 1975; Schellman, 1978), we calculated the $\Delta G°$, m, and $C_{1/2}$ values listed in Table 2. The similarities in the value of m for the different amino acid substitutions suggest that the balance of effects in the folded and unfolded states is roughly similar for all the mutants (Shortle & Meeker, 1986; Shortle et al., 1990), a result consistent with our use of the same two-state model for analyzing each transition. The $\Delta G°$ data in Table 2 allow us to define the following order of stabilities for the eight mutants: C30V/C51A > C30A/C51A > C30T/C51A ≅ C30S/C51A > C30G/C51A ≅ C30A/C51S > C30S/C51S > C30G/C51M.

van't Hoff Transition Enthalpies as a Function of pH. To assess the dependence of ΔH_{VH} on temperature and thus estimate ΔC_p, we measured and analyzed CD denaturation profiles for selected mutants at different pH values, which

Table 3: Calorimetrically Measured Thermodynamic Parameters for Melting of the 30−51 Disulfide Mutants of BPTI at pH 7

	BPTI (wt)[a]	BPTI (wt)[b]	C30A/C51A[c]	C30V/C51A[c]	C30G/C51A[c]	C30T/C51A[d]	C30S/C51A[c]	C30A/C51S[c]
T_m (°C)	104	104.5	71 ± 0.5	72 ± 0.5	57 ± 0.5	62 ± 0.5	61 ± 0.5	56 ± 0.5
ΔT_m (°C)			33	32	47	42	43	48
$\Delta H°_d$ (kcal/mol)	70	74.6	59.4 ± 4.0	59.5 ± 4.0	51.9 ± 4.0	52.4 ± 4.0	55.7 ± 3.5	50.4 ± 4.0
$\Delta S°_d$ [cal/(mol·K)]	186		173 ± 12	172 ± 12	157 ± 12	156 ± 12	167 ± 10	153 ± 12
$\Delta H°_{VH}$ (kcal/mol)	70	77.5	64.8 ± 4.5	58.9 ± 5.0	54.6 ± 4.0	53.9 ± 5.0	56.6 ± 4.5	57.5 ± 5.0
r ($\Delta H_{VH}/\Delta H_d$)	1	1.04	1.09	0.99	1.05	1.02	1.02	1.44

[a] Schwarz et al., 1987. [b] Makhatadze et al., 1993 (data were measured at pH 4.9). [c] Multiple measurements were performed. Errors are obtained from standard deviations. [d] Single measurements were performed. Errors are obtained from fitting.

results in an unfolding transition at different T_m values. The resulting ΔH_{VH} and T_m data are plotted in panel A of Figure 4. Note that, for all the mutants, we found ΔH_{VH} to be an approximately linear function of T_m between pH 2 and 7, a result consistent with a temperature-independent ΔC_p value. From the slope of this line, we calculated ΔC_p, the CD-derived difference in the heat capacity between the folded and unfolded states. These ΔC_p values are listed in the final column of Table 1.

Differential Scanning Calorimetry. To gain further insight into the basis for the substitution-induced alterations in BPTI properties, we also used differential scanning calorimetry (DSC) to study a subset of the 30−51 disulfide mutants. Figure 5 shows a representative DSC thermogram for the C30S/C51A mutant, while Table 3 lists the thermodynamic parameters we have derived by analysis of the calorimetric melting profiles for the six mutants studied. Inspection of these data and those in Table 2 reveals several features worthy of note. First, the calorimetric T_m data (Table 3) indicate that all the mutants are thermally destabilized relative to wild type BPTI, with this thermal destabilization ranging from 32 to 48 °C. Although some of the T_m differences are close to the error limit, this calorimetric-based order of thermal stability is the same as that derived from the CD data, with the absolute T_m values being somewhat different, as one would expect for a comparison of T_{max} and T_m data (Gralla & Crothers, 1973). Second, the denaturation enthalpies, $\Delta H°_d$, of the mutants (Table 3), at the respective T_m's, are substantially reduced by between 10 and 20 kcal/mol relative to wild type BPTI. Thus, the substitution-induced decrease in T_m is entirely enthalpic in origin. In fact, the substitutions actually result in a slight entropy-induced stabilization of the mutants relative to the wild type at the respective T_m's, a contribution which is more than compensated for by the enthalpy term. We have made these ΔH and ΔS comparisons at the melting temperatures, which are different for the wild type and mutants, simply to compare the driving forces at the respective T_m values. A more direct comparison would require use of ΔC_p data to compare the values at a common reference temperature. Third, despite these significant substitution-induced decreases in T_m and ΔH for each transition upon removal of the 30−51 disulfide bond, the ratios of the van't Hoff and calorimetric enthalpies remain near unity. This latter observation implies that, independent of the substituted residues, removal of the disulfide bond has little effect on the cooperativity of the thermal denaturation, a result consistent with the assumption employed in our analysis of the optical data that all the mutants undergo denaturation via two-state transitions.

Calorimetric Enthalpies as a Function of pH and ΔC_p Values. To determine the dependence of ΔH_d on T_m, we used DSC to measure the thermally induced denaturation enthalpy for each BPTI mutant at different pH values, while recognizing the potential hazard(s) of such an analysis as recently emphasized by Sturtevant (1994). The results of these measurements are plotted in panel B of Figure 4. For all the mutants studied, we found ΔH_d to be a linear function of T_m between pH 2 and 7, a result consistent with a temperature-independent ΔC_p value. From the slope of these plots, we calculated ΔC_p, the difference in heat capacity between the folded and the unfolded states (Shortle et al., 1988; Connelly et al., 1991). These ΔC_p values are listed in Table 4, along with the calorimetrically measured thermodynamic parameters for each mutant. Comparison be-

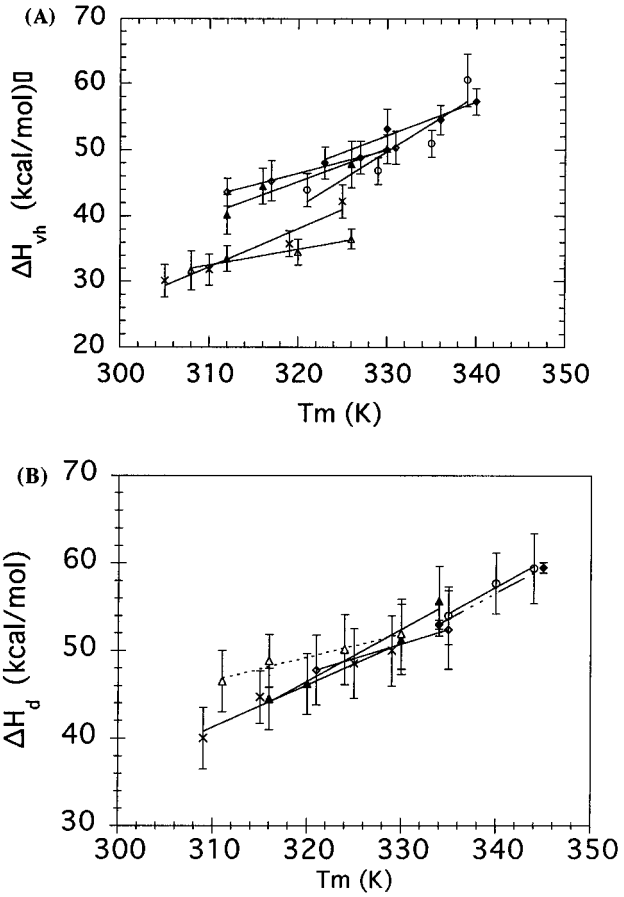

FIGURE 4: (A) ΔH_{VH} of 30−51 disulfide mutants (measured from CD melting) as a function of melting temperature: C30A/C51A (open circles); C30V/C51A (filled diamonds); C30G/C51A (open triangles); C30T/C51A (open diamonds); C30S/C51A (filled triangles); C30A/C51S (×). ΔH_{VH}'s were estimated from thermally induced denaturations monitored by CD at different pHs in order to alter T_m. (B) $\Delta H°_d$ of 30−51 disulfide mutants (measured from DSC) as a function of melting temperature: C30A/C51A (open circles); C30V/C51A (filled diamonds); C30G/C51A (open triangles); C30T/C51A (open diamonds); C30S/C51A (filled triangles); C30A/C51S (×). $\Delta H°_d$'s were measured at different pHs to alter T_m.

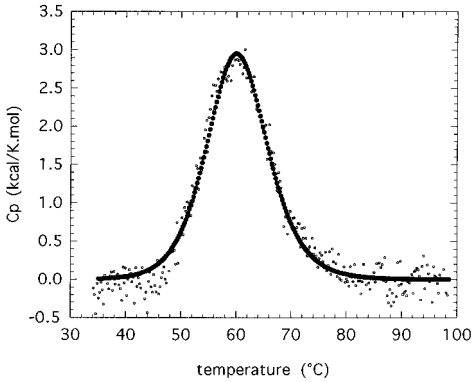

FIGURE 5: Example of a DSC thermogram for the denaturation of the 30−51 disulfide mutant C30S/C51A, measured in 10 mM potassium phosphate (pH 7.0) and 100 mM NaCl.

Table 4: Calorimetrically Measured Thermodynamic Data Extrapolated to 25 °C for the Unfolding of the 30−51 Disulfide Mutants of BPTI

proteins	$\Delta H°_d$ (kcal/mol)	$\Delta S°_d$ [cal/(mol·K)]	$\Delta G°_d$ (kcal/mol)	ΔC_p [kcal/(mol·deg)]
C30A/C51A	29.5 ± 5.0	80 ± 12	5.8 ± 0.3	0.65 ± 0.2
C30V/C51A	31.8 ± 5.0	86 ± 12	6.1 ± 0.3	0.59 ± 0.2
C30G/C51A	43.6 ± 2.3	130 ± 12	4.6 ± 0.1	0.26 ± 0.2
C30T/C51A	40.2 ± 3.3	118 ± 10	5.1 ± 0.1	0.33 ± 0.2
C30S/C51A	34.5 ± 3.6	100 ± 10	4.8 ± 0.2	0.59 ± 0.2
C30A/C51S	36.5 ± 2.1	108 ± 12	4.1 ± 0.1	0.45 ± 0.2

Table 5: Comparison of the pH 7 Unfolding Free Energies, $\Delta G°$, of the 30−51 Disulfide Mutants of BPTI at 25 °C Obtained from Thermal Denaturation Data Monitored by CD ($\Delta G°_{CD}$) and DSC ($\Delta G°_{DSC}$) and from Optically Detected, Denaturant-Induced Unfolding ($\Delta G_{denaturant}$)

mutant	$\Delta G°_{CD}$ (kcal/mol)	$\Delta G°_{DSC}$ (kcal/mol)	$\Delta G°_{denaturant}$ (kcal/mol)
C30A/C51A	5.3	5.8	5.5
C30V/C51A	5.7	6.1	6.6
C30G/C51A	3.9	4.6	3.2
C30T/C51A	4.4	5.1	4.5
C30S/C51A	4.1	4.8	4.4
C30A/C51S	3.0	4.1	3.4
C30S/C51S	2.6	−	2.7
C30G/C51M	1.7	−	2.1

tween the ΔC_p data in Tables 1 and 4 reveals qualitative agreement between the values derived optically and calorimetrically. This agreement is reasonably good considering the rather significant errors associated with these analyses. Using the calorimetrically determined T_m, ΔH_d, and ΔC_p values at pH 7, we have calculated $\Delta G°$ (25 °C), the unfolding free energy at 25 °C using the Gibbs−Helmholtz equation. These values are listed in the penultimate column of Table 4.

DISCUSSION

Relative Stabilities of the 30−51 Disulfide Mutants. Table 5 lists the unfolding free energies for the 30−51 disulfide mutants determined using the three different methods employed in this study, namely, Gdn-HCl-mediated denaturation ($\Delta G_{denaturant}$), as well as thermally induced denaturation monitored by CD (ΔG_{CD}) and by DSC (ΔG_{DSC}). The plots shown in Figure 6 present an overall comparison of these three sets of ΔG data. The observed linear relationships indicate that the $\Delta\Delta G$ values measured by these independent methods are highly correlated. One interpretation of this correlation is that the free energies of the denatured states—whether produced by Gdn-HCl-mediated unfolding or thermal denaturation—are, under the experimental conditions used, similar for this set of mutants. A similar high degree of concordance between free energy changes measured by Gdn-HCl denaturation and those estimated from differential scanning calorimetry was observed in a study of various cavity-creating mutations in the hydrophobic core of chymotrypsin inhibitor 2 (Jackson et al., 1993). Our results expand on those of Jackson et al. (1993) by showing that the agreement between these different methods extends to polar as well as hydrophobic substitutions.

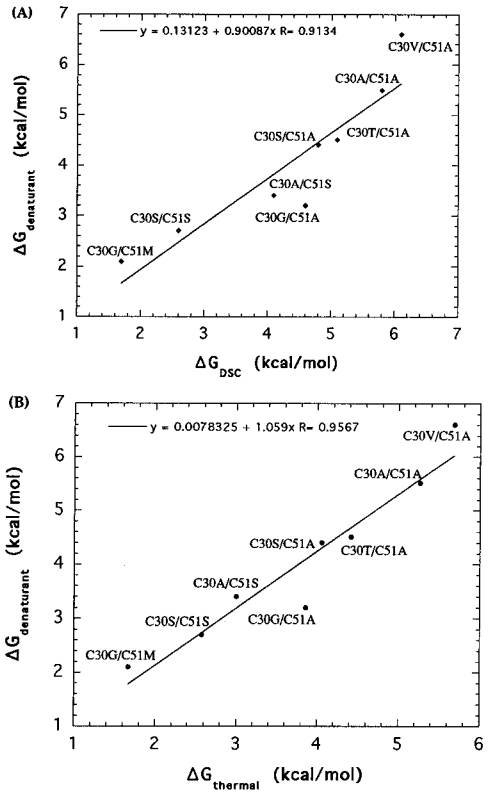

FIGURE 6: (A) Correlation between the unfolding free energies (ΔG) for the 30−51 disulfide mutants of BPTI obtained from Gdn-HCl-induced denaturation monitored by CD and from thermally induced denaturation measured by DSC. The solid line shows the best linear fit of two sets of ΔG data for eight 30−51 disulfide mutants. Using estimated ΔC_p, the "ΔG_{DSC}" data for mutants C30S/C51S and C30G/C51M were extrapolated from ΔH and T_m values measured by CD melting (Tables 1 and 5). The slope and intercept of the line are given by the equation at the top of the panel. (B) Correlation between the unfolding free energies (ΔG) for the 30−51 disulfide mutants of BPTI obtained from Gdn-HCl-induced denaturation monitored by CD and from thermally induced denaturation measured by CD. The solid line shows the best linear fit of two sets of ΔG data for eight 30−51 disulfide mutants. The slope and intercept of the line are given by the equation at the top of the panel.

The difference in the unfolding free energy change between a mutant and a reference protein, $\Delta\Delta G°$, is given by the relationship $\Delta\Delta G°_d = \Delta G°_d(\text{mutant}) - \Delta G°_d(\text{ref})$ (Dao-pin et al., 1991; Connelly et al., 1991). The value of $\Delta\Delta G°_d$ provides a measure of the change in apparent stability induced in a reference protein by specific amino acid substitution(s). In this work, we define the C30A/C51A mutant as our reference protein. The first two data columns of Tables 6−8 list the $\Delta\Delta G$ values we have calculated in this manner for specific types of substitutions. In the sections

Table 6: Influence of Polarity on the Thermodynamic Impact of the Substituted Residue

mutant	$\Delta\Delta G°_{Gdn}$[a] (kcal/mol)	$\Delta\Delta G°_{DSC}$[b] (kcal/mol)	$\Delta\Delta H°_{DSC}$[b] (kcal/mol)	$\Delta\Delta S°_{DSC}$[b] [cal/(mol·K)]
C30A/C51A	0	0	0	0
C30V/C51A	0.5	0.3	2.3	6.4
C30S/C51A	−1.8	−1.0	5.0	20.0
C30T/C51A	−1.5	−0.7	10.7	38.3

[a] Calculated at the midpoints of the denaturation curves where $\Delta G = 0$ and $\Delta G° = mC_{1/2}$ (eq 6) from the m and $C_{1/2}$ values for each mutant given in Table 2. See Jackson et al. (1993). [b] From the DSC data in Table 4.

Table 7: Thermodynamic Impact of Structural Context on Ala → Ser Substitutions

mutant	$\Delta\Delta G°_{Gdn}$[a] (kcal/mol)	$\Delta\Delta G°_{DSC}$[a] (kcal/mol)	$\Delta\Delta H°_{DSC}$[a] (kcal/mol)	$\Delta\Delta S°_{DSC}$[a] [cal/(mol·K)]
C30A/C51A	0	0	0	0
C30S/C51A	−1.8	−1.0	5.0	20.0
C30A/C51S	−2.4	−1.7	7.0	28.3
C30S/C51S	−3.3	nd[b]	nd[b]	nd[b]

[a] See legend to Table 6. [b] Not determined.

Table 8: Thermodynamic Impact of Glycine and Methionine Substitutions

mutant	$\Delta\Delta G°_{Gdn}$[a] (kcal/mol)	$\Delta\Delta G°_{DSC}$[a] (kcal/mol)	$\Delta\Delta H°_{DSC}$[a] (kcal/mol)	$\Delta\Delta S°_{DSC}$[a] [cal/(mol·K)]
C30A/C51A	0	0	0	0
C30G/C51A	−2.7	−1.2	14.1	50.3
C30G/C51M	−4.0	nd[b]	nd[b]	nd[b]

[a] See legend to Table 6. [b] Not determined.

that follow, we discuss how the nature of the substituted residues influences their effects on protein stability.

Polarity of the Substituted Residue and Its Impact on Protein Stability—comparison of Mutants A30/A51, S30/A51, V30/A51, and T30/A51. Since the 30 and 51 sites are buried in the hydrophobic core of the protein, the stabilities of the 30−51 disulfide mutants should be influenced by the polarity of the amino acid(s) replaced. The $\Delta\Delta G$ data in Table 6 reveal that substitutions in the core at position 30 by the polar residues serine or threonine cause a decrease in protein stability relative to the reference protein. Specifically, replacement of −H by −OH in the residue 30 side chain (an alanine to serine substitution) reduces the protein stability by 1.0−1.8 kcal/mol. Replacement of $-CH_3$ by an −OH group on the β carbon in the Val30 to Thr30 mutation causes a 1.0−2.0 kcal/mol decrease in the stability of C30T/C51A relative to C30V/C51A. The upper range of this decrement in the unfolding free energy is in good agreement with the $\Delta\Delta G$ estimate of −2.0 kcal/mol for this mutant pair determined by Hurle et al. (1990) using the change in tyrosine absorbance to monitor unfolding.

By contrast with the destabilizing consequences of inserting a polar residue into the core at position 30, inspection of the C30V/C51A data in Table 6 reveals that insertion of the hydrophobic residue valine in place of alanine actually induces an *increase* in stability relative to the reference protein, an observation consistent with a previous study (Hurle et al., 1990). In fact, the $\Delta\Delta G$ values of +0.5 and +0.3 kcal/mol determined here for the valine substitution using CD-monitored Gdn-HCl-induced unfolding and DSC measurements, respectively, are in good agreement with the previously reported value of +0.5 kcal/mol derived from the denaturant-dependent absorbance change at 287 nm (Hurle et al., 1990, 1992). Inspection of the enthalpy data in Table 6 ($\Delta\Delta H$ value of +2.3 kcal/mol) reveals that the valine substitution-induced stabilization at 25 °C is entirely enthalpic in origin. By contrast, the corresponding $\Delta\Delta H$ data for the serine and threonine mutants reveal that, relative to the A30/A51 reference protein, the destabilization induced by these substitutions at 25 °C is entirely entropic in origin.

The loss of side chain conformational entropy during protein folding, especially for buried core residues in relatively rigid regions of the native polypeptide, recently has been recognized as an important destabilizing influence in the balance of enthalpic and entropic terms which contribute to the free energy of the folded protein (Doig & Sternberg, 1995). The calculated mean destabilizations (at 25 °C) due to this effect for serine, threonine, and valine relative to alanine are −1.1, −1.1, and −0.4 kcal/mol, respectively (Pickett & Sternberg, 1993; Abagyan & Totrov, 1994; Creamer & Rose, 1994; Koehl & Delarue, 1994; Lee et al., 1994; Doig & Sternberg, 1995). Inspection of the data in Table 6 reveals that the magnitude of this calculated side chain conformational entropy loss is comparable to the entire destabilization we observe for the C30S/C51A vs C30A/C51A comparison and approximately half of the destabilization we observe for the C30T/C51A vs C30V/C51A comparison. Thus, the effects on the free energy of stabilization caused by the Ala → Ser and Val → Thr substitutions are not solely due, *per se*, to burial of polar groups in the hydrophobic core.

The data listed in Table 6 reveal that the difference in $\Delta G°$ between C30A/C51A and C30S/C51A is approximately the same as that between C30V/C51A and C30T/C51A. Because the side chain volume of alanine is smaller than that of cysteine, replacement of cysteines 30 and 51 by alanines causes a correlated movement of the two chain segments toward each other to compensate partially for the packing defect (Eigenbrot et al., 1990). Since the side chain volumes of serine, valine, and threonine are similar to that of cysteine, they may fill more completely than can alanine the cavity left by removal of cysteine 30. This feature may lessen the rearrangement of the main chain and the neighboring side chains, thereby partly compensating for the decrease in stability due to the insertion of a polar −OH group in the core and the loss of side chain conformational entropy. Recently, the energetic costs and structural consequences of burying a hydroxyl group in the core of T4 lysozyme have been assessed by comparing Ala to Ser and Val to Thr substitutions (Blaber et al., 1993). In general, the structural perturbations were found to be minor, and the $\Delta\Delta G$ values for such mutations varied between 1.0 and 2.8 kcal/mol, a range consistent both with our results and with data for polar substitutions in the core of barnase (Serrano et al., 1992).

Influence on Protein Stability of the Structural Context of the Mutated Residue. The C30S/C51A and C30A/C51S mutants both substitute serine and alanine for the two half-cystines of the 30−51 disulfide bond, but with opposite orientations of the two residues with respect to the substituted disulfide. The data in Table 7 provide a comparison of the thermodynamic parameters we have determined relative to the C30A/C51A reference protein for these two mutants and for the C30S/C51S double mutant. Inspection of these data reveals that the contribution to the free energy of stabilization

of the substituted residue is related not only to the nature of the amino acid substitution but also, in part, to the structural context. Residue 51 is located in the middle of an α-helix, and residue 30 is located in a β-sheet (Eigenbrot et al., 1990). It is well known that amino acids have distinct conformational preferences that can stabilize or destabilize an α-helix (Chou & Fasman, 1978), with alanine being the most helix-favoring of the 20 common amino acids (Lyu et al., 1989; O'Neil & Degrado, 1990; Bryson et al., 1995). Serine, on the other hand, usually is considered to be helix destabilizing because the side chain hydroxyl can compete with main chain amides for hydrogen bonding with carbonyls, thereby disrupting the backbone H-bonding of the helix (Richardson & Richardson, 1988; Presta & Rose, 1988). Our data (Table 7) are consistent with both of these conformational preferences in that we find substitution of serine for alanine at residue 30 (in the β-sheet) to be less destabilizing by 0.6−0.7 kcal compared with substitution of serine for alanine at residue 51 (in the α-helix). Interestingly, host−guest studies on model peptides have estimated the difference in the free energy of α-helix stabilization, $\Delta\Delta G_\alpha$, between alanine and serine to be 0.3−0.8 kcal/mol (O'Neil & Degrado, 1990; Lyu et al., 1990; Bryson et al., 1995), in reasonably good agreement with our data, although admittedly the comparison is imperfect. Despite the quantitative positional differences noted above, our data reveal a serine for alanine substitution at either site to be destabilizing by approximately 1−2 kcal. Our calorimetric data show this substitution-induced destabilization to be entirely entropic in origin.

Additional contributions to the difference in $\Delta G°$ between the C30S/C51A and the C30A/C51S mutants may arise from subtle disparities between the local environments around the two mutation sites due to differences in neighboring side chain and main chain atoms. An example of such local environmental effects is found in studies of Ala to Ser and Val to Thr mutations in T4 lysozyme which revealed the cost of burying a hydroxyl group to be reduced if a hydrogen-bonding partner was available (Blaber et al., 1993). Thus, in our work, the C30S/C51S BPTI "double serine" mutant might be expected to exhibit greater stability than either of the "single serine" mutants due to the potential for side chain−side chain H-bond formation between the two serine residues. However, our data (Table 7) reveal the stabilization free energy, $\Delta\Delta G$, for this mutant to be roughly additive: the $\Delta\Delta G$ for the double serine mutant approaches the sum of the $\Delta\Delta G$'s for the two single serine mutants. In the absence of fortuitous compensations, this feature suggests that the interaction between the two serine side chains in this mutant is not strong (Wells, 1990). To examine this possibility further, we modeled the C30S/C51S mutant structure by homology using as a basis the X-ray structure of the C30A/C51A mutant (Eigenbrot et al., 1990). This modeling exercise indicated that the Ser30 and Ser51 hydroxyl groups could not be oriented in a way that was consistent with strong H-bonding interactions without distorting the structure (results not shown). If one were to force a hydrogen bond between these two −OH groups, the resulting strain would most likely result in a higher energy state.

The free energy additivity we observe for the two serine residues also is crudely reflected in the thermal melting data, although, in principle, it need not be manifest in this observable. Compared with the reference mutant, C30A/C51A, the T_m of the double serine mutant C30S/C51S is lower by 20 °C, which is also approximately the sum of the decrease for mutant C30S/C51A and C30A/C51S (Table 1). Recently, two groups have studied BPTI variants containing only a single disulfide, [C14A/C38A, C30A/C51A] and [C14S/C38S, C30S/C51S] (Staley & Kim, 1992; Mierlo et al., 1991). Staley and Kim (1992) reported the T_m of the mutant [C14A/C38A, C30A/C51A] to be approximately 40 °C, while Mierlo et al. (1991) reported the T_m of the mutant [C14S/C38S, C30S/C51S] to be approximately 15 °C. Neglecting the different substitutions of cysteines 14 and 38, which have only minor differential effects on stability (Liu, Breslauer, and Anderson, unpublished results), the ΔT_m of 25 °C between [C14A/C38A, C30A/C51A] and [C14S/C38S, C30S/C51S] is in good agreement with the ΔT_m value we observe in this work between C30A/C51A and C30S/C51S (Table 1).

Effect of Glycine and Methionine Substitutions at the 30−51 Disulfide Site. Inspection of the data in Table 8 reveals that mutants with glycine substitutions at residue 30 are highly destabilized relative to the C30A/C51A reference protein. In a comprehensive study of destabilizing mutations of staphylococcal nuclease, where *both* alanine and glycine were substituted at numerous positions in the core of the protein, a glycine mutation at any position was found to be 1.7−3.6 kcal/mol more destabilizing than the corresponding alanine mutation at that position (Shortle & Meeker, 1986, 1989; Shortle et al., 1990; Shortle, 1992). This range of values is consistent with the $\Delta\Delta G$ of 1.2−2.7 kcal/mol that we observe here for the G30/A51 mutant versus the A30/A51 mutant.

Any attempt to rationalize our glycine substitution data (or for that matter, any of the results presented here) must consider substitution-induced effects on both the native and the denatured states. In this connection, Sturtevant (1994) has noted that "...it is in general difficult, if not impossible, to assign ... thermodynamic changes caused by mutations to either the initial state, or the final state...". Although we agree with this assertion, we will attempt to discuss possible ways in which a glycine substitution might influence initial and final states. Since glycine does not have a side chain, substitution of a glycine at residue 30 might cause a packing defect in the core of the folded protein, an event that could result in a destabilizing increase in free energy for the native state of up to 2 kcal/mol [see Huang et al. (1995)]. Furthermore, the high flexibility of glycine might cause an increase in the configurational entropy of the unfolded state of mutant C30G/C51A, thereby resulting in a decrease in its free energy (Nemethy et al., 1966). This latter expectation is consistent with our entropy data (Table 8) in that the C30G/C51A mutant exhibits the highest entropy of unfolding at 25 °C for any of the mutants studied here.

Glycine mutations are not always more destabilizing than the corresponding alanine mutations. For example, at residue 43 of BPTI (an asparagine in the wild type molecule), a glycine substitution mutant was found to be *more* stable than the alanine mutant at this same position (Goldenberg et al., 1989; Kim et al., 1993). This phenomenon has been attributed to solvation effects in the relatively hydrophilic cavity vacated by the Asn side chain (Danishefsky et al., 1993).

We have used similar cavity packing considerations in an attempt to build more stability into a Gly30-substituted BPTI

mutant. To this end, we made and tested the C30G/C51M BPTI mutant. Our expectation was that the unbranched methionine side chain with two methylene groups, a sulfur, and a methyl group might adopt a relatively unstrained conformation nearly isosteric to that of the missing disulfide and perhaps neatly "thread" the cavity between residue 30 and residue 51 Cα carbons. Contrary to this expectation, our data show that this mutant is severely destabilized by 4.0 kcal relative to the reference protein (Figures 3 and 4, Table 8). As a possible trivial explanation, we considered fortuitous methionine oxidation during workup of the protein, since burial of a relatively polar and more bulky sulfoxide- or sulfone-bearing side chain in the hydrophobic core could cause significant destabilization. This possibility, however, was ruled out by high-resolution mass spectrometry (Materials and Methods) which yielded a mass for the mutant consistent with a protein containing unoxidized methionines.

A plausible explanation for the relative instability of the C30G/C51M mutant is the effect on side chain conformational entropy caused by the Ala → Met substitution at residue 51. The loss of conformational entropy is a major force that opposes protein folding. Recently, Doig and Sternberg (1995) compared folding-related changes in side chain conformational entropy for all 20 amino acids at 300 K, using estimates provided by various groups (Pickett & Sternberg, 1993; Abagyan & Totrov, 1994; Koehl & Delarue, 1994; Creamer & Rose, 1994; Lee et al., 1994). The mean value of $T\Delta S_{conf}$ for methionine relative to alanine upon unfolding was 1.5 kcal/mol due to the large number of degrees of freedom of the linear methionine side chain which are "frozen out" when the side chain is buried in the core (Doig & Sternberg, 1995). Such a destabilization due to the A51M mutation plus the destabilization caused by an Ala to Gly mutation at residue 30 (2.7 kcal/mol, Table 8) yields a predicted decrease in the stability of the C30G/C51M mutant relative to the C30A/C51A mutant of 4.2 kcal/mol. This is very close to the experimental value of 4.0 kcal/mol (Table 8). However, in the absence of any structural data, significant rearrangements of both side chain and backbone atoms relative to their respective positions in wild type BPTI cannot be ruled out for this mutant; such "repacking" of protein cores can alter stability in unexpected ways (Lim et al., 1994).

Impact of Mutations on the Unfolding Enthalpy. As noted above, the denaturation enthalpies, $\Delta H°_d$, of the 30−51 disulfide mutants are lower by about 10−20 kcal/mol compared to that of wild type BPTI (Table 3). The denaturation enthalpies of the A30/A51 and V30/A51 mutants, although close to the error limits, appear to be higher than those of the other four 30−51 disulfide mutants, while being similar to each other. This similarity may reflect similar patterns of hydrogen bonding and hydration of the core residues for these two mutants. In fact, X-ray crystallographic analyses have demonstrated the conformations of wild type BPTI and the C30A/C51A and the C30V/C51A mutants to be very similar (Hurle et al., 1992; Eigenbrot et al., 1990, 1992). Thus, if one crudely assumes isoenthalpic final states, the difference in denaturation enthalpy between wild type BPTI (74 kcal/mol) at its T_m and the A30/A51 (or V30/A51) mutants (59 kcal/mol) at their T_m's may be used to approximate the net stabilizing enthalpic impact of the 30−51 disulfide bridge to be about 15 kcal/mol. This analysis, however, is fraught with assumptions, including not comparing the enthalpy data at a common temperature, that at best render this estimate a starting point for further discussions.

Correlations between Folding-Induced Changes in Water-Accessible Surface Area and ΔC_p. The changes in the heat capacity observed during the folding of globular proteins are thought to be related to a reduction in the water-accessible nonpolar surface area of the protein (Livingstone et al., 1991; Privalov & Khechinashvili, 1974; Privalov, 1979; Spolar et al., 1989; Dec & Gill, 1985). Recent work (Makhatadze & Privalov, 1990; Murphy & Gill, 1991; Spolar et al., 1992) has shown that the burial of polar surface area upon protein folding also contributes to the heat capacity change. Spolar et al. (1992) have derived an empirical equation[2] for calculating this heat capacity change which includes the average contributions of folding-induced changes in polar (ΔA_p) and nonpolar (ΔA_{np}) surface area:

$$\Delta C_p = (0.32 \pm 0.04)\Delta A_{np} + (-0.14 \pm 0.02)\Delta A_p \quad (8)$$

Murphy and Gill (1991) have derived a similar equation:[2]

$$\Delta C_p = (0.45 \pm 0.02)\Delta A_{np} + (-0.26 \pm 0.03)\Delta A_p \quad (9)$$

In both expressions, ΔA_{np} and ΔA_p are the changes in nonpolar and polar surface area, respectively, which accompany protein folding. Our calculations (see Materials and Methods) of the amounts of water-accessible polar and nonpolar surface area buried upon folding of the mutants studied here indicate that about 75 ± 1% of the total change in water-accessible surface area is nonpolar and 25 ± 1% is polar. Consequently, changes in both polar and nonpolar surface area contribute to the change in heat capacity, with the burial of nonpolar surface being the dominant contributor.

Because the relative proportions of buried polar vs nonpolar surfaces were affected to only a minor extent by the amino acid substitutions studied, our calculated ΔC_p°'s all fell within a relatively narrow range: 0.45 ± 0.01 kcal/(mol·K) (using eq 8) and 0.59 ± 0.01 kcal/(mol·K) (using eq 9).[3] These calculated values both agree, within experimental error, with the ΔC_p's we have measured for the 30−51 disulfide mutants using CD-monitored thermal denaturation (mean ΔC_p = 0.50 kcal/(mol·K), range = 0.24−0.84; Table 1) and differential scanning calorimetry (mean ΔC_p = 0.48 kcal/(mol·K), range = 0.26−0.65; Table 4). Thus, the two experimentally determined mean ΔC_p values agree remarkably well with each other and with the theoretical ΔC_p values calculated by the two methods noted above. This agreement is particularly satisfying considering the rather *ad hoc* manner in which we derived the random coil structures for the surface area calculations (Materials and Methods) and the substantial errors inherent in the experimental ΔC_p determinations (Figure 4). Theory predicts that ΔC_p should be relatively insensitive to the differences in the particular amino acid substitutions examined (see above), suggesting that the spread of ΔC_p values we observe is primarily due to experimental uncertainties in the ΔH

[2] The area differentials are in units of Å^2, and the coefficients have units of cal mol^{-1} K^{-1} Å^{-2}.

[3] For the purpose of these calculations, sulfur was assumed to be a polar atom (see Materials and Methods). However, cystine sulfurs can also be considered as nonpolar atoms [see Lesser and Rose (1990)]. This would have the effect of increasing both of the calculated ΔC_p's only slightly [0.02−0.03 kcal/(mol·K)].

measurements rather than reflective of intrinsic mutant-specific ΔC_p differences.

CONCLUDING REMARKS

In this work, we have used spectroscopic and calorimetric techniques to characterize the consequences on protein properties of amino acid substitutions at positions 30 and 51 of BPTI, which contain the two half-cystine residues of the 30−51 disulfide in the native protein. Our goal was to gather data that might reveal some general principles for rationally "designing out" a buried disulfide bridge in a manner that results in a predictable impact on protein stability. We viewed this primarily as a didactic exercise aimed at illuminating the unique features of disulfide bonds as stabilizing moieties in proteins. In this design phase, we limited our initial efforts to substitutions at residues 30 and 51. However, a more general solution to this problem would be to also vary those surrounding residues that have side chains which pack against the 30−51 disulfide bond in wt BPTI [see, for example, Waldburger et al. (1995), and Desjarlais and Handel (1995)].

Disulfide stabilization of proteins has traditionally been attributed to two main effects: (a) reduction of the configurational entropy of the unfolded state due to cross-bridging of the polypeptide chain and (b) van der Waals and hydrophobic packing interactions (especially for buried disulfides) in the native state (Betz, 1993). Our attempts to compensate for the loss of the disulfide cross-link by means of noncovalent interactions involving alternative residues at the 30 and 51 positions revealed several principles. First, an attempt to restore stability via a putative Ser 30−Ser 51 side chain−side chain H-bonding interaction failed: the serines caused further instability due to burial of the polar side chain in the hydrophobic core environment and loss of side chain conformational entropy, with the geometry of the interaction precluding strong hydrogen bond formation. Second, attempts to pack the cavity with a number of nonhydrogen, non-polar side chain atoms equivalent to those found in the missing disulfide (Cys + Cys = 2 + 2 = 4) revealed a Val−Ala combination (3 + 1) to be far superior to a Gly−Met combination (0 + 4), even though the latter pair employed an unbranched linear side chain sterically analogous to the disulfide bond. We interpreted this destabilization to result from a combination of entropic effects that lowered the energy of the unfolded state, by increasing the configurational entropy of the main chain due to the glycine substutition and the side chain conformational entropy due to the methionine substitution. Our results, in fact, point to a third, previously unrecognized, property of disulfides that may contribute to their stabilizing effects on proteins; namely, *their relatively restricted side chain rotational freedom in the unfolded state*. This property endows cystine residues (and perhaps sterically hindered adjacent residues as well) with a relatively modest $T\Delta S_{conf}$ penalty upon folding to the native state (Doig & Sternberg, 1995).

The microscopic interpretations we have presented here of our macroscopic data are intended to provide bases for further discussions, rather than to represent singular explanations of the molecular origins of the thermodynamic and extrathermodynamic properties we have measured. As has been noted by Sturtevant (1994), "It is absolutely clear that we are far from a firm understanding of the primarily noncovalent forces that hold proteins in their native structures, and that achieving such an understanding lies far in the future. This situation makes it more important to give much attention to accumulating reliable thermodynamic data concerning all aspects of protein behavior." We concur with this assessment and believe that the results presented in this paper make a meaningful contribution toward the goal of accumulating reliable thermodynamic data on protein systems.

ACKNOWLEDGMENT

We are grateful to Björn Nilsson for the gift of pEZZ318 and for suggesting the use of *E. coli* strain RV308. We thank Li Chung Ma and Seho Kim for helpful discussions regarding expression and refolding issues. We benefited from the generosity of Phyllis Kosen and Irwin Kuntz (UCSF), who provided samples of some of the mutant proteins used in the early phases of this work. We are also indebted to Ron Levy for making available to us his software for performing the simulations of the unfolded state.

REFERENCES

Abagyan, R., & Totrov, M. (1994) *J. Mol. Biol. 235*, 983−1002.
Altman, J. D., Henner, D., Nilsson, B., Anderson, S., & Kuntz, I. D. (1991) *Protein Eng. 4*, 593−600.
Betz, S. F. (1993) *Protein Sci. 2*, 1551−1558.
Blaber, M., Lindstrom, J. D., Gassner, N., Xu, J., Heinz, D. W., & Matthews, B. W. (1993) *Biochemistry 32*, 11363−11373.
Breslauer, K. J. (1994) *Methods Mol. Biol. 26*, 347−72.
Breslauer, K. J. (1995) *Methods Enzymol. 259*, 221−242.
Bryson, J. W., Betz, S. F., Lu, H. S., Suich, D. J., Zhou, H. X., O'Neil, K. T., & DeGrado, W. F. (1995) *Science 270*, 935−941.
Chakrabartty, A., Kortemme, T., Padmanabhan, S., & Baldwin, R. L. (1993) *Biochemistry 32*, 5560−5565.
Chothia, C. (1975) *Nature 254*, 304−308.
Chou, P. Y., & Fasman, G. D. (1978) *Adv. Enzymol. 47*, 45−148.
Connelly, P., Ghosaini, L., Hu, C., Kitamura, S., Tanaka, A., & Sturtvent, J. (1991) *Biochemistry 30*, 1887−1891.
Creamer, T. P., & Rose, G. D. (1994) *Proteins: Struct., Funct., Genet. 19*, 85−97.
Danishefsky, A., Housset, D., Kim, K.-S., Tao, F., Fuchs, J., Woodward, C., & Wlodawer, A. (1993) *Protein Sci. 2*, 577−587.
Dao-pin, S., Anderson, D. E., Baasa, W. A., Dahlquist, F. W., & Matthews, B. W. (1991) *Biochemistry 30*, 11521−11529.
Davaloo, P., & Crothers, D. M. (1976) *Biochemistry 15*, 5299−5305.
Dec, S. F., & Gill, S. J. (1985) *J. Solution Chem. 14*, 417−429.
Desjarlais, J. R., & Handel, T. M. (1995) *Protein Sci. 4*, 2006−2018.
Dill, K. A. (1990) *Science 250*, 297−298.
Doig, A. J., & Sternberg, M. J. E. (1995) *Protein Sci. 4*, 2247−2251.
Edelhoch, H. (1967) *Biochemistry 6*, 1948−1954.
Eigenbrot, C., Randal, M., & Kossiakoff, A. A. (1990) *Protein Eng. 3*, 591−598.
Eigenbrot, C., Randal, M., & Kossiakoff, A. A. (1992) *Proteins: Struct., Funct., Genet. 14*, 75−87.
Eriksson, A. E., Baase, W. A., Zhang, X.-J., Heinz, D. W., Blaber, M., Baldwin, E. P., & Matthews, B. W. (1992) *Science 255*, 178−183.
Ferrer, M., Borany, G., & Woodward, C. (1995) *Nat. Struct. Biol. 2*, 211−217.
Garvey, E. P., & Matthews, C. R. (1989) *Biochemistry 28*, 2083−2093.
Goldenberg, D. P., Frieden, R. W., Haack, J. A., & Morrison, T. B. (1989) *Nature 338*, 127−132.
Gralla, J., & Crothers, D. M. (1973) *J. Mol. Biol. 73*, 497−511.

Huang, K., Lu, W., Anderson, S., Laskowski, M. J., & James, M. N. G. (1995) *Protein Sci. 4*, 1985−1997.
Hurle, M., Anderson, S., & Kuntz, I. D. (1991) *Protein Eng. 4*, 451−455.
Hurle, M. R., Marks, C. B., Kosen, P. A., Anderson, S., & Kuntz, I. D. (1990) *Biochemistry 29*, 4410−4419.
Hurle, M. R., Eads, C. D., Pearlman, D. A., Seibel, G. L., Thomason, J., Kosen, P. A., Kollman, P., Anderson, S., & Kuntz, I. D. (1992) *Protein Sci. 1*, 91−106.
Jackson, S. E., Maracci, M., elMasry, N., Johnson, C. M., & Fersht, A. R. (1993) *Biochemistry 32*, 11259−11269.
Kassell, B. (1970) *Methods Enzymol. 19*, 844−852.
Kellis, J. T. J., Nyberg, K., & Fersht, A. R. (1989) *Biochemistry 28*, 4914−4922.
Kim, K.-S., Tao, F., Fuchs, J., Danishefsky, A., Housset, D., Wlodawer, A., & Woodward, C. (1993) *Protein Sci. 2*, 588−596.
Kim, S., Baum, J., & Anderson, S. (1997) *Protein Eng.* (in press).
Kitchen, D. B., Hirata, F., Westbrook, J. D., Levy, R. M., Kofke, D., & Yarmush, M. (1990) *J. Comput. Chem. 11*, 1169−1177.
Koehl, P., & Delarue, M. (1994) *J. Mol. Biol. 239*, 249−275.
Ladbury, J. E., Wynn, R., Thomson, J. A., & Sturtevant, J. M. (1995) *Biochemistry 34*, 2148−2152.
Lee, B., & Richards, F. M. (1971) *J. Mol. Biol. 55*, 379−340.
Lee, K. H., Xie, D., Freire, E., & Amzel, L. M. (1994) *Proteins: Struct., Funct., Genet. 20*, 68−84.
Lesser, G. J., & Rose, G. D. (1990) *Proteins: Struct. Funct., Genet. 8*, 6−13.
Lim, W. A., & Sauer, R. T. (1989) *Nature 339*, 31−6.
Lim, W. A., Farruggio, D., & Sauer, R. T. (1992) *Biochemistry 31*, 4324−4333.
Lim, W. A., Hodel, A., Sauer, R. T., & Richards, F. M. (1994) *Proc. Natl. Acad. Sci. U.S.A. 91*, 423−427.
Livingstone, J. R., Spolar, R. S., & Record, M. T., Jr. (1991) *Biochemistry 30*, 4237−4244.
Lyu, P. C., Marky, L. A., & Kallenbach, N. R. (1989) *J. Am. Chem. Soc. 111*, 2733.
Lyu, P. C., Liff, M. I., Marky, L. A., & Kallenbach, N. R. (1990) *Science 250*, 669−673.
Makhatadze, G., & Privalov, P. L. (1990) *J. Mol. Biol. 213*, 375−384.
Makhatadze, G., Kim, K.-S., Woodward, C., & Privalov, P. L. (1993) *Protein Sci. 2*, 2028−2036.
Manning, M. C., & Woody, R. W. (1989) *Biochemistry 28*, 8609−8613.
Marks, C. B., Vassar, M., Ng, P., Henzel, W., & Anderson, S. (1986) *J. Biol. Chem. 261*, 7115−7118.
Marks, C. B., Naderi, H., Kosen, P. A., Kuntz, I. D., & Anderson, S. (1987a) in *Protein Structure, Folding and Design* (Oxender, D., & Fox, C. F., Eds.) Vol. 2, pp 335−340, Alan R. Liss, Inc., New York.
Marks, C. B., Naderi, H., Kosen, P. A., Kuntz, I. D., & Anderson, S. (1987b) *Science 235*, 1370−1371.
Marky, L. A., & Breslauer, K. J. (1987) *Biopolymers 26*, 1601−1620.
Mauer, R., Meyer, B. J., & Ptashne, M. (1980) *J. Mol. Biol. 139*, 147−161.
Mierlo, C. P. M., Darby, N. J., Neuhaus, D., & Creighton, T. E. (1991) *J. Mol. Biol. 222*, 373−390.
Murphy, K. P., & Gill, S. J. (1991) *J. Mol. Biol. 222*, 699−709.
Nemethy, G., J., L. S., & Scheraga, H. A. (1966) *J. Phys. Chem. 70*, 998−1004.
Nilsson, B., & Abrahmsen, L. (1990) *Methods Enzymol. 185*, 144−161.
Nilsson, B., Forsberg, G., & Hartmanis, M. (1991a) *Methods Enzymol. 198*, 3−16.
Nilsson, B., Marks, C. B., Kuntz, I. D., & Anderson, S. (1991b) *J. Biol. Chem. 266*, 2970−2977.
O'Neil, K. T., & Degrado, W. F. (1990) *Science 250*, 646−651.
Pace, C. N. (1975) *CRC Crit. Rev. Biochem. 3*, 1−43.
Pace, C. N., Laurents, D. V., & Thomson, J. A. (1990) *Biochemistry 29*, 2564−2572.
Pickett, S. D., & Sternberg, M. J. E. (1993) *J. Mol. Biol. 231*, 825−839.
Ponder, J. W., & Richards, F. M. (1987) *J. Mol. Biol. 193*, 775−791.
Presta, L. G., & Rose, G. D. (1988) *Science 240*, 1632−1641.
Privalov, P. L. (1979) *Adv. Protein Chem. 33*, 167−241.
Privalov, P. L., & Khechinashvili, N. N. (1974) *J. Mol. Biol. 86*, 665−684.
Richards, F. M. (1974) *J. Mol. Biol. 82*, 1−14.
Richards, F. M. (1977) *Annu. Rev. Biophys. Bioeng. 6*, 11−176.
Richards, F. M., & Lim, W. A. (1994) *Q. Rev. Biophys. 26*, 423−498.
Richardson, J. S., & Richardson, D. C. (1988) *Science 240*, 1648−1652.
Sambrook, J., Fritsch, E. F., & Maniatis, T. (1989) *Molecular Cloning, a Laboratory Manual*, 2nd ed., Cold Spring Harbor Laboratory Press, Cold Spring Harbor, NY.
Sanger, F., Nicklen, S., & Coulson, A. R. (1977) *Proc. Natl. Acad. Sci. U.S.A. 74*, 5463−5467.
Santoro, M. M., & Bolen, D. W. (1988) *Biochemistry 27*, 8063−8068.
Sayers, J. R., Schmidt, W., & Eckstein, F. (1988) *Nucleic Acids Res. 16*, 791−802.
Schellman, J. A. (1978) *Biopolymers 17*, 1305−1322.
Schwarz, H., Hinz, H.-J., Mehlich, A., Tschesche, H., & Wenzel, H. (1987) *Biochemistry 26*, 3544−3551.
Serrano, L., Kellis, J. T. J., Cann, P., Matouschek, A., & Fersht, A. R. (1992) *J. Mol. Biol. 224*, 783−804.
Shortle, D. (1992) *Q. Rev. Biophys. 25*, 205−250.
Shortle, D., & Meeker, A. K. (1986) *Proteins 1*, 81−89.
Shortle, D., & Meeker, A. K. (1989) *Biochemistry 28*, 936−944.
Shortle, D., Meeker, A. K., & Freire, E. (1988) *Biochemistry 27*, 4761−4768.
Shortle, D., Stites, W. E., & Meeker, A. K. (1990) *Biochemistry 29*, 8033−8041.
Spolar, R. S., Ha, J.-H., & Record, M. T., Jr. (1989) *Proc. Natl. Acad. Sci. U.S.A. 86*, 8382−8385.
Spolar, R. S., Livingstone, J. R., & Record, M. T., Jr. (1992) *Biochemistry 31*, 3947−3955.
Staley, J. P., & Kim, P. S. (1992) *Proc. Natl. Acad. Sci. U.S.A. 89*, 1519−1523.
Sturtevant, J. M. (1994) *Curr. Opin. Struct. Biol. 4*, 69−78.
Vieira, J., & Messing, J. (1987) *Methods Enzymol. 153*, 3−11.
Vuilleumier, S., Sancho, J., Loewenthal, R., & Fersht, A. R. (1993) *Biochemistry 32*, 10303−10313.
Waldburger, C. D., Schildbach, J. F., & Sauer, R. T. (1995) *Struct. Biol. 2*, 122−128.
Wells, J. A. (1990) *Biochemistry 29*, 8509−8517.
Yang, J. T., & Kubota, S. (1985) in *Microdomains in Polymer Solutions* (Dubin, P. L., Ed.) p 311, Plenum Press, New York, NY.

BI962423C